High-frequency Heating Behavior of Veneer-based Composites: Modelling and Validation

Peixing Wei,[a] Brad Jianhe Wang,[b] Chunping Dai,[b] Siwei Huang,[a] Xin Rao,[c] Wending Li,[a] and Dingguo Zhou [a,*]

A one-dimensional theoretical heat and mass transfer model was developed for high-frequency (HF) heating of veneer-based composites, such as laminated veneer lumber (LVL) and plywood. This model was based on the basic principles of energy and mass conservation, momentum conservation of gas flow, and gas thermodynamic relations. The response variables, including temperature, gas pressure, and moisture content (MC), were linked to basic material properties, such as veneer density, thermal conductivity, permeability, and dielectric properties. Initial and boundary conditions for solving the governing equations were also considered. The model was further validated by experiments with veneer HF heating and LVL HF heating. The model predictions agreed well with the experimental results. During veneer HF heating, the inner veneer core layers had lower MC than the outer surface layers. Compared to conventional hot platen heating, HF heating was proven to be an efficient and robust method for manufacturing veneer-based composites.

Keywords: High-frequency (HF) heating; Veneer-based composites; Heat and mass transfer; Model

*Contact information: a:College of Materials Science and Engineering, Nanjing Forestry University, Nanjing, P. R. China 210037; b: Engineered Wood Products Manufacturing Department, FPInnovations-Wood Products, 2665 East Mall, Vancouver, B.C., Canada V6T1Z4; c: Jiangsu Polytechnic College of Agriculture and Forestry, Zhenjiang, P. R. China 212400; *Corresponding author: dgzhou@njfu.com.cn.*

INTRODUCTION

From a manufacturing standpoint, hot-pressing is a critical step in the manufacturing of veneer-based composites whereby a resinated veneer assembly is heated and consolidated (Wang 2007). Glue coated on the veneer surface requires a certain quantity of heat energy to polymerize and to form veneer-to-veneer bonds. Thus, hot pressing not only affects manufacturing productivity, but also determines panel quality. During the conventional hot platen pressing, heat is sequentially transferred from the platen to the panel core primarily through heat conduction and convection (Bolton *et al.* 1989 a, b; Dai and Yu 2004; Deng *et al.* 2006; Humphrey and Bolton 1989; Thöemen and Humphrey 2003; Zombori *et al.* 2002). The densities of the pressed composites across the vertical direction are usually non-uniform, *i.e.*, higher density in the surface layers and lower density in the core. This well-known vertical density profile (VDP) is a result of the temporal and spatial interactions between heat and mass transfer and of panel consolidation (Dai and Yu 2004). Hot platen pressing requires extremely long times for heat to transfer from the surface to the core, particularly when pressing thick veneer-based composites.

An interesting alternative to hot pressing is electromagnetic (EM) heating. Since the energy is delivered directly to the whole assembly, the heat transfer is not just relying on the conduction from the surface (Pereira *et al.* 2004). EM radiation is usually divided into high-frequency (HF) and microwave (MW). Despite MW having higher frequencies than HF, these two frequency bands are often blurred and hard to demarcate. Nevertheless, HF and MW dielectric heating can be distinguished by installation. The HF heating system uses high power electrical values, transmission lines, and applicators in the forms of capacitors, whereas the microwave system uses magnetrons, waveguides, and resonant (or non-resonant) cavities (Jones and Rowley 1996). The choice of HF or MW radiation is determined by the dimensions of the object to be heated (Roussy and Pearce 1995). EM heating has been used for about 60 years in the wood-processing industry for drying, bending, and gluing of wood; additionally, modern-day improvements in EM heating equipment make this technology particularly well suited for polymer curing in the manufacture of wood-based panels (Pereira *et al.* 2004). There are some distinct advantages in using this type of heating as pre-heating or co-heating of wood-based panels, such as: the reduction of the press cycle, the synchronization of glue curing through the thickness, and the uniformity of vertical density (Maloney 1989). Thus, EM heating presents a good alternative to the manufacturing of thicker and more uniform wood products (Pereira *et al.* 2004).

The application of EM heating for solid wood drying has been studied theoretically and experimentally by many investigators (Resch 2006). Although EM heating is widely used for the manufacture of wood-based panels, there have been few relevant studies published in the scientific literature (Deng *et al*. 2006; Pereira *et al*. 2004; Resnik *et al*. 1997). Some HF heating studies have revealed both positive and negative effects on final panel properties when using this technology (Fahey 1976; Woodson and Stevens 1977). In comparison with conventional hot platen pressing, fiberboard made by HF heating has better machinability and coating ability, higher dimensional stability and internal bond, and improved edge screw holding and hardness. Because of its more uniform VDP, the final product has slightly lower bending strength and stiffness. Deng *et al.* (2006) carried out an experimental study of the MW pre-heating of a medium-density fiberboard (MDF) mat, which focused on the moisture and the temperature distribution within the mat. The results showed that the MW pre-heating not only increases the overall mat temperature with high energy efficiency within a very short period of time, but also redistributes the mat moisture. And this redistribution creates a potentially favorable moisture gradient, namely, moisture content (MC) gradually lowering from the surface to the inner. Further, Pereira *et al*. (2004) developed a three-dimensional model to reveal the HF heating mechanism of MDF. However, owing to different elements of wood used, the heat and mass transfer of veneer-based composites is different from that of non veneer-based composites (*i.e.*, MDF) (Wang 2007).

Since mathematical models can help better understand the hot-pressing process of wood-based panels, various simulation models with different levels of complexity have been developed, particularly for non veneer-based composites (Bolton and Humphrey 1994; Carvalho and Costa 1998; Dai 2001; Dai and Yu 2004; Dai *et al*. 2005, 2007; Humphrey and Bolton 1989; Kelly 1977; Lenth and Kamke 1996; Thöemen and Humphrey 2006; von Haas *et al*. 1998; von Haas and Fruhwald 2000, 2001; Wang and Winstorfer 2000; Yu *et al*. 2007). Wang (2007) was the first to study the conventional hot pressing behavior of veneer-based composites. While focusing on the mechanism of heat and mass transfer, a one-dimensional model was developed to predict temperature, MC,

gas pressure, and density across the assembly during hot pressing. Unfortunately, this model is unable to predict the heat and mass transfer when employing HF heating because of different energy source.

Experimental and numerical methods have been widely used to study the hot-pressing behavior of wood-based panels. The experimental methods offer the possibility of direct measurements of temperature and gas pressure inside the mats by sensor technology during hot pressing (Wang 2007) and help improve general understanding of the hot-pressing process. However, the internal conditions of a large industrial panel are difficult to measure in a mill environment. Compared to model predictions, experimental methods are time-consuming and not cost-effective (Dai *et al*. 2007). Furthermore, traditional metallic sensors are unable to measure *in situ* temperature and other variables during HF heating or pre-heating process of wood-based panels.

In spite of HF heating technique being widely used for manufacturing wood-based panels, very limited work has been reported on the experimental and modelling investigations of the HF heating or pre-heating process (Pereira *et al*. 2004; Deng *et al*. 2006). In this paper, a one-dimensional theoretical model to simulate the heat and mass transfer was developed to improve the fundamental understanding of the HF heating behavior of veneer-based composites. And then, some experiments were conducted to validate the model.

MODEL DEVELOPMENT

Conceptualization of Veneer-based Composites

According to previous work (Wang *et al*. 2006), the compression ratio (CR) is the most important factor affecting panel permeability. In terms of decreasing importance, the next factors are the veneer sapwood/heartwood composition, the glue spread level, and the degree of glue curing. So the glueline in the veneer-based composites did not act as the primary barrier to heat convection for gas or moisture movement and CR was the main concern in this work. To simplify the model, a glue-covered veneer layer was seen as a control element without differentiating the glueline and the wood veneer layer. Due to its laminated structure, the veneer-based composites can be conceptualized as a chain series of control elements (*i.e.*, glue-covered veneer layers), as shown in Fig.1.

General Hypothesis and Simplifications

For veneer-based composites, the length and width are generally much larger than the thickness. It can be assumed that heat transfer mainly occurs in the thickness direction (Yu 2011). Owing to the practical application of thickness control, the thickness of the veneer-based composites remains constant during the hot pressing process. A fundamental one-dimensional heat and mass transfer model was developed based upon the following assumptions:

1. Each control element (*i.e.*, glue-covered veneer layer) is viewed as a mixture of three constituents: dry wood, moisture, and glue solids;
2. The heat and water produced by the glue polymerization reactions are negligible;
3. The dielectric parameters of each control element primarily change due to the variation of MC and temperature, and the polymerization of the glue; and
4. During hot pressing, the heat transfer occurs *via* both heat conduction and convection.

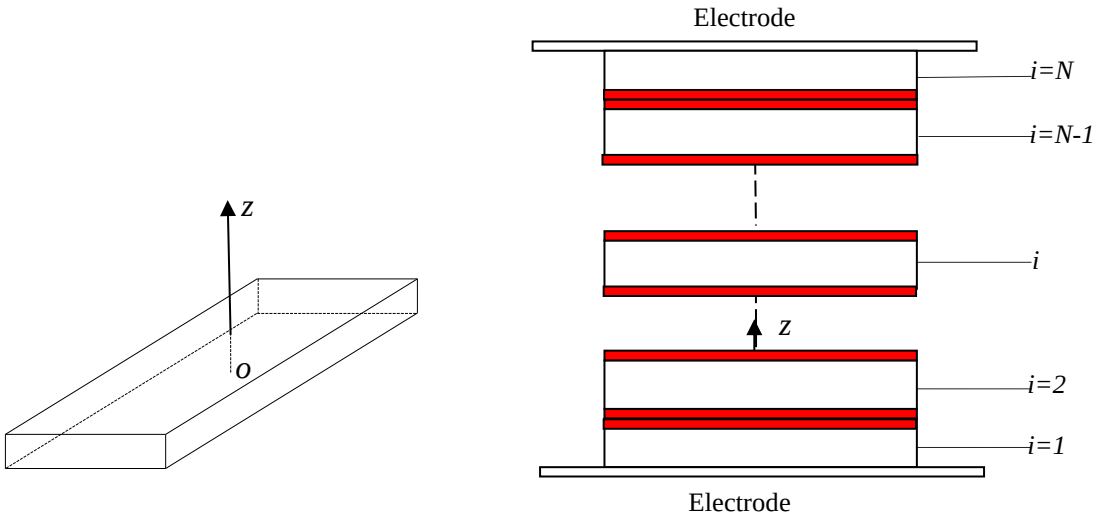

Fig. 1. A typical veneer-based composites assembly (***i*** −glue-covered veneer layer number; ***N*** −total number of veneer layers)

Heat and Mass Transfer

Heat conservation

During HF heating, the control element (*i.e.*, glue-covered veneer layer) absorbs EM energy, and its temperature change is governed by heat conduction, heat convection, and heat loss caused by water vaporization. By the energy conservation law, the transient energy balance for a control element within the assembly can be expressed as (Yu 2011),

$$\frac{\partial \rho_v c_v T}{\partial t} = \Phi_v + k_v \frac{\partial^2 T}{\partial z^2} + \frac{\partial \rho_g c_g u_{z,g} T}{\partial z} - \dot{E}_{ev,v} H_{fg} \quad (1)$$

where ρ_v is the density of the control element (kg/m^3); c_v is the specific heat of the control element (J/kg•K); T is the temperature of the control element (K); Φ_v is the heat generation rate (J/m^3•s) of the control element during HF heating; k_v is the thermal conductivity (W/m•K) of the control element; ρ_g is the density of gas phase; c_g is the specific heat of gas (mixture of air and water vapor); $u_{z,g}$ is the effective gas velocity (m/s); $\dot{E}_{ev,v}$ is the water evaporation rate of the control element (kg/m^3•s); H_{fg} is the latent heat of water vapor (kJ/kg); and z is the unit dimension in the panel thickness direction.

Mass conservation

The mass of each control element is mainly the sum of the dry wood, glue solids and moisture. Thus, the density of the control element can be expressed as,

$$\rho_v = \rho_d + \rho_d MC_v \quad (2)$$

where MC_v is the MC within the control element based upon the wood oven dry weight; and ρ_d is the dry wood and glue solids density (kg/m^3), which is constant without considering the transient mechanical deformation during hot pressing. The derivative of

Eq.2 with respect to time, which expresses the change in the density of the control element, is:

$$\frac{d\rho_v}{dt} = \rho_d \frac{dMC_v}{dt} \quad (3)$$

Thus, Eq. 3 reveals that density variations of the solids within the veneer are only caused by changes of MC due to its mass transfer. This equation can be rearranged to incorporate the moisture evaporation rate, $\dot{E}_{ev,v}$ (kg/m^3•s):

$$-\rho_d \frac{dMC_v}{dt} = \dot{E}_{ev,v} \quad (4)$$

In the control element, the gas is a mixture of air and water vapor inside the voids. The density of the gas is the sum of air volume density (ρ_{air}) and vapor volume density (ρ_{vapor}), or:

$$\rho_g = \rho_{air} + \rho_{vapor} \quad (5)$$

It should be noted that ρ_{air} is generally dependent upon the void space and the lateral air permeability. The value of ρ_{air} can be assumed to be constant with an average value of 1kg/m^3 due to the relatively large lateral air permeability during pressing (Wang 2007).

Assuming that the vapor velocity is the same as the air or gas velocity, the mass balance of water vapor can then be written as (Yu 2011),

$$\varphi \frac{\partial \rho_{vapor}}{\partial t} + \frac{\partial \rho_{vapor} u_{z,g}}{\partial z} = \dot{E}_{ev,v} \quad (6)$$

where φ is the void fraction (%), and $u_{z,g}$ is the effective gas velocity (m/s), which is governed by the gas momentum equations discussed in the following section.

Momentum conservation of gas flow

The velocity of gas flow obeys the gas momentum law for porous media, *i.e.*, the well-known Darcy's Law (Yu 2011),

$$u_{z,g} = -\frac{K_v}{\mu} \frac{dP_g}{dz} \quad (7)$$

where K_v is the permeability of the control element (m^2) and μ is the dynamic viscosity (Pa•s) of the gas (water vapor and air), which varies with the local temperature (1.846×10^{-5} Pa•s at 20 °C). The parameter P_g is the gas pressure (Pa), which is governed by the gas thermodynamics relation discussed in the following section.

Gas pressure

Gas is a mixture of air and water vapor (Yu 2011). According to Dalton's Law, the total pressure of a gas mixture is equal to the sum of the partial pressures of its constituents. In the present case, the gas pressure should be the sum of the partial pressures of air (P_{air}) and water vapor (P_{vapor}) expressed as (Dai and Yu 2004),

$$P_g = P_{air} + P_{vapor} \quad (8)$$

The gas pressure is the main concern during HF heating. When the gas pressure in the panel is too high, the panel will be delaminated easily while the platen is open and thus affects the panel integrity and quality (Wang 2007). According to the gas state equation, air partial pressure within the control element can be calculated as follows:

$$P_{air} = \frac{\rho_{air} RT}{M_{air}} \quad (9)$$

where ρ_{air} is the air volume density (kg/m^3); R is the universal gas content (8.315 J/mol•K); M_{air} is the molecular weight of air (29.0 g/mol); and T is the temperature (K).

Similarly, the relationship between water vapor density ρ_{vapor} and its pressure P_{vapor} is as follows,

$$\rho_{vapor} = \frac{P_{vapor} M_{vapor}}{RT} \quad (10)$$

where M_{vapor} is the molecular weight of water (18.02 g/mol). Further, by the definition of relative humidity (RH) of moist air, the water vapor pressure can be calculated by,

$$P_{vapor} = RH \cdot P_{sat} \quad (11)$$

where P_{sat} is the saturated vapor pressure (MPa), which is only dependent on the temperature (T). The relationship between these two variables is typically given in a standard steam table, or can be calculated by the following equation (Siau 1995):

$$P_{sat} = exp\left\{53.421 - \frac{6516.3}{T} - 4.125 \cdot ln(T)\right\} \quad (12)$$

Assuming local equilibrium, the relationship between the MC of the control element, the RH, and the temperature can be obtained based upon the Gibbs free energy equation (Nelson 1983),

$$RH = exp\left\{-\frac{M_{vapor}}{RT} exp\left[ln(\Delta G_0)\left(1.0 - \frac{MC_v}{FSP}\right)\right]\right\} \quad (13)$$

where FSP is the fiber saturated point (30%); and ΔG_0 is the Gibbs free energy per mass unit of absorbed water (J/kg), which can be viewed as a constant with the value of 693.627×10^3 J/kg (Nelson 1983).

Equations (8) through (13) reveal the inherent gas thermodynamics relationships involved with HF heating of veneer-based composites.

EM Energy Conversion to Heat

The dielectric capacity of the material, in combination with the EM field, results in EM energy converted to heat. The transmitted power to an object may be calculated using the Poynting Vector ($\boldsymbol{P}(t)$) (Bucki and Perré 2003; Roussy and Pearce 1995),

$$\boldsymbol{P}(t) = \boldsymbol{E}(t) \times \boldsymbol{H}(t) \quad (14)$$

where $\boldsymbol{E}$ is the electric vector field vector (V/m); $\boldsymbol{H}$ is the magnetic field vector (A/m); and t is the heating time (s).

The Poynting vector describes the local power density absorbed by the material in a propagating wave. Its direction shows the propagation path, and the power density flux accounts for the vector's magnitude. Previous models in this field of research often have assumed that all the volume possessed a uniform electric field (Bucki and Perré 2003). The following simplified equation is generally used for the absorbed power per unit volume of a material,

$$\Phi_v = \omega \varepsilon_0 \varepsilon'' E_{eff}^2 = 5.56 \times 10^{-11} f \varepsilon'' E_{eff}^2 \quad (15)$$

where Φ_v is the absorbed power per unit volume of the material (w/m^3 or J/m^3•s); ω is the angular frequency (rad/s), which is equal to $2\pi f$; f is the radiation frequency (Hz); ε_0 is the free space permittivity, which is equal to 8.85×10^{-12}F/m; and ε'' is the relative dielectric loss factor. The term E_{eff} is the effective electric field intensity (V/m), which is calculated as follows,

$$E_{eff} = \frac{U}{h} \quad (16)$$

where U is the applied voltage (V); and h is the gap between the top electrode and the bottom electrode (m). The gap value h is equivalent to the thickness of the veneer-based composites in this work.

Obviously, the energy absorbed by each volume element is a function of the local material dielectric properties, the electric field intensity, and the EM field frequency.

Wood dielectric parameter

The speed and degree to which wood can be heated under HF conditions depend on many factors. These factors include cell structure, physical and chemical properties, MC, temperature, and the grain direction with respect to the direction of the electromagnetic field (Torgovnikov 1993). Previous investigations have shown that wood MC has the greatest influence on the dielectric parameter, followed by temperature (James 1977; Kröner and Pungs 1953; Pound 1959; Torgovnikov 1993). As a consequence, the experimental data presented by Torgovnikov (1993) were adopted by some investigators (Bucki and Perré 2003; Pereira *et al.* 2004). Based on the empirical equation obtained by Pereira *et al.* (2004), the relative dielectric loss factor of wood can be expressed as,

$$\varepsilon''_{wood} = 0.0178 \cdot exp(2.32T^* + 21.95MC) \quad (17)$$

with T^* defined as $(T - T_{min})/(T_{max} - T_{min})$, where T is the wood temperature (°C); T_{min} is the minimum temperature (20 °C); and T_{max} is the maximum temperature (150 °C); and MC represents the wood's moisture content (%).

Glue dielectric parameter

The degree of glue curing is the ratio of the final mass of the cured glue to the initial mass of the uncured glue. The general equation, adapted from Dai and Yu (2004), is as follows,

$$\frac{d\alpha}{dt} = A_0(1-\alpha)^n \cdot exp\left(-\frac{\Delta E}{RT}\right) \quad (18)$$

where α is the degree of glue curing; t is the heating time (s); n is the order of the chemical curing reaction; A_0 is the collision factor (1/s); ΔE is the activation energy (J/mol), which can be obtained through experiments; and R is the universal gas constant, 8.315J/mol·K.

Sernek and Kamke (2007) used least square regression of laboratory data to obtain the values of the parameters of Eq.18:

$$\frac{d\alpha}{dt} = 9.15 \times 10^5 \cdot (1-\alpha)^{1.48} \cdot exp\left(-\frac{5877}{T}\right) \quad (19)$$

Glue is converted from the liquid to the solid state by chemical reaction and removal of water evaporation (Odian 2004). Sernek and Kamke (2007) conducted a dielectric analysis for continuous in-press monitoring of the curing of phenol-formaldehyde (PF) glue, and obtained an approximate relationship between the relative dielectric loss factor of the glue (ε''_{glue}) and the degree of glue curing (α) based upon the experimental data,

$$\varepsilon''_{glue} \approx \varepsilon''_{glue,0}(1-\alpha) \quad (20)$$

where $\varepsilon''_{glue,0}$ is the relative dielectric loss factor of the uncured liquid glue, which can be obtained from the literature. The value of this parameter for PF glue is about 140 (Cheng 1985; Lu 1986; Shen 1983; Yin 1996).

Combining Eqs.17 and 20, the relative dielectric loss factor of control element in Eq.(15) can be calculated by the following equation,

$$\varepsilon'' = \varepsilon''_{wood} + \varepsilon''_{glue} \quad (21)$$

NUMERICAL SOLUTION OF THE MODEL

Finite Difference Method

The differential equation of heat transfer of the control element can be discretized to a difference equation (Wang 2007). As shown in Fig. 1, the energy conservation can then be expressed using the following difference equation for the i^{th} control element as,

$$T_{v,i}^{n+1} = T_{v,i}^{n} + \frac{1}{c_{v,i}\rho_{v,i}h_{v,i}}\left\{\Phi_{v,i} + k_{v,i}\frac{2(T_{i+1}^{n}-T_{i}^{n})}{h_{v,i+1}+h_{v,i}} + k_{v,i}\frac{2(T_{i-1}^{n}-T_{i}^{n})}{h_{v,i-1}+h_{v,i}} + c_{g,i}\rho_{g,i}u_{z,g,i}^{n}\frac{2(T_{i+1}^{n}-T_{i}^{n})}{h_{v,i+1}+h_{v,i}} - \dot{m}_{ev,v}\cdot H_{fg}\right\}\Delta t$$

and

$$\Phi_{v,i} = \omega\varepsilon_0\varepsilon''_{v,i}E^2_{v,i}h_{v,i} = 5.56\times10^{-11}f\varepsilon''_{v,i}E^2_{v,i}h_{v,i};$$

$$\dot{m}_{ev,v} = \dot{E}_{ev,v}\cdot h_{v,i},\ i=2,\ \ldots,\ N\text{-}1 \qquad (22)$$

where n+1 represents the current time, and n represents the previous time; $T_{v,i+1}$ and $T_{v,i}$ are respectively the temperature of the i+1th and the i^{th} control element; $c_{v,i}$ and $c_{g,i}$ are the specific heats of the i^{th} control element veneer layer and the gas, respectively; $\rho_{v,i}$ and $\rho_{g,i}$ are the density of the i^{th} control element and the gas, respectively; $u_{z,g,i}$ is the effective gas velocity of the i^{th} control element; $h_{v,i+1}$ and $h_{v,i}$ are respectively the thickness of the i+1th and i^{th} control element; $k_{v,i}$ is the heat conductivity of the i^{th} control element; $\Phi_{v,i}$ is the heat generation rate (J/m^2•s) of the i^{th} control element during HF heating; and $\dot{m}_{ev,v}$ is the water evaporation rate of the i^{th} control element (kg/m^2•s). Similarly, based on the above derivations, the MC governing equation of the i^{th} control element can also be expressed using the difference equation as:

$$MC^{n+1}_{v,i} = MC^n_{v,i} - \frac{1}{\rho_d h_{v,i}}\left(\varphi\frac{\rho^{n+1}_{vapor,i}-\rho^n_{vapor,i}}{\Delta t} + u^n_{z,g,i}\frac{\rho^n_{vapor,i+1}-\rho^n_{vapor,i}}{h_{v,i}} + \rho^n_{vapor,i}\frac{u^n_{z,g,i+1}-u^n_{z,g,i}}{h_{v,i}}\right)\Delta t \qquad (23)$$

Note that H_{fg} is the latent heat of evaporation, which ranges from 2100 to 2450kJ/kg for temperatures ranging from 20 to 150 °C (Incropera and Dewitt 1990).

According to Siau (1995), k_v, the thermal conductivity of the veneer layer, is a function of the veneer layer density and its MC:

$$k_{v,i} = 0.024 + 0.001\times\rho_{v,i}\times(0.2+0.38\times MC_i) \text{ for } i = 1,2,\ldots,N \qquad (24)$$

where $\rho_{v,i}$ is the veneer's density for the i^{th} layer; and MC_i is the veneer's MC for the i^{th} layer.

Additionally, the specific heat of the veneer layer is a function of the veneer's MC, which can be expressed as:

$$c_{v,i} = 84 + (1113 + MC_i\times4186)/(1+MC_i) \text{ for } i = 1,2,\ldots,N \qquad (25)$$

So far, Eqs. 22 and 23 are the basic governing equations for heat and mass transfer of HF heating of veneer-based composites.

Special Conditions

Initial conditions

Initial values of variables are summarized as follows:

1. Before HF heating, the temperature of veneer assembly is the same as the ambient temperature; and
2. Initial gas flow velocity: $u_{z,g,0} = 0$.

Geometric conditions

According to the assumptions, veneer-based composites can be seen as N layers of glue-covered veneers (*i.e*., N control elements).

Boundary conditions

While the press is closed until it is opened for decompression, the following boundary condition exists:

$$u_{zg} = 0 \text{ when } \begin{cases} z = 0 \\ z = h \end{cases} \quad (26)$$

Given that the top and bottom surfaces of an assembly are in perfect thermal contact with the platen, the interface thermal resistance is zero and there is no temperature difference across the interface.

In the HF heating of veneer-based composites, one common boundary condition with thermally insulated electrode at both sides is applied. This is a modification of the "heated electrodes" method, which does not require any source of external heat. Instead of the massive pressure platens of the press, thin sheets of conductive material are used as electrodes and backed up by a suitable layer of thermal insulation. This layer should also be of high-quality electrical insulation to isolate the electrodes from the structure of the press. When the electrodes have a low thermal capacity as compared to the material being heated, the percentage heat loss into the platens is negligible.

For the surface control elements (*i*=1 or N), the energy balance equation can be simplified (*i.e.*, *i*=1):

$$\Phi_{v,1} + k_{v,1}\frac{(T_{v,2}-T_{v,1})}{h_{v,1}} = \frac{d\left(c_{v,1}\rho_{v,1}h_{v,1}T_{v,1}\right)}{dt} + \dot{m}_{ev,v}\cdot H_{fg} \quad (27)$$

In this expression, $T_{v,1}$ and $T_{v,2}$ are the temperature of the first control element (*i*=1), and the second control element (*i*=2), respectively; $c_{v,1}$ is the specific heat of the first control element; $\rho_{v,1}$ is the density of the first control element; $h_{v,1}$ is the thickness of the first control element; $k_{v,1}$ is the thermal conductivity of the first control element; $\Phi_{v,1}$ is the heat generation rate of the first control element.

SIMPLIFICATION OF THE MODEL DURING HF HEATING OF VENEER-BASED COMPOSITES

Contribution of Heat Convection during HF Heating of Veneer-based Composites

Figure 2 shows the predicted temperature rise of a laminated veneer lumber (LVL) assembly (with a CR=5%) by considering convection and by ignoring convection based on the air permeability data of aspen veneer from the previous work (Wang 2007). It is apparent from the two close curves that heat convection had little influence on the heat transfer during HF heating of the LVL assembly. Hence, heat convection or gas movement along the vertical direction should be negligible when a CR of 5 to 15% is employed during the manufacturing of veneer-based composites.

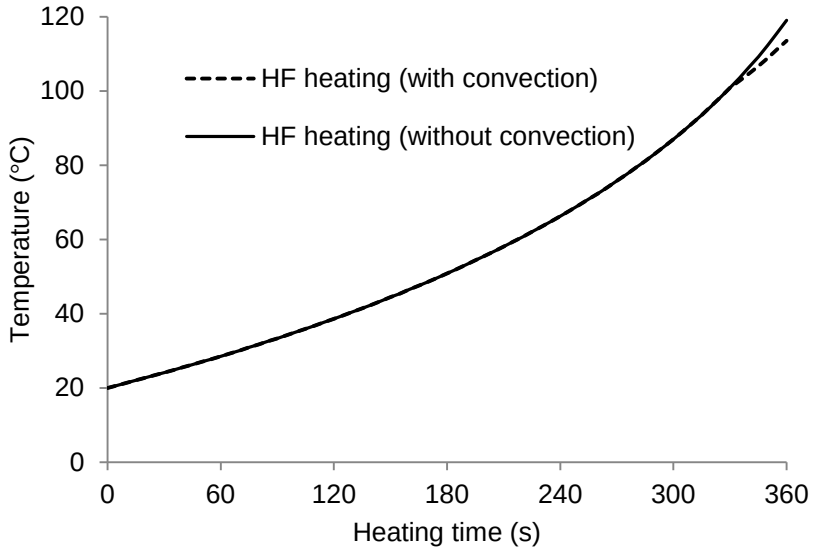

Fig. 2. Temperature increase predictions of HF heating of a LVL assembly by considering and by ignoring convection

Simplified Mathematical Solutions of the Model

If heat convection or gas movement is neglected during HF heating of veneer-based composites, then Eq.(22) can be simplified as follows:

$$T_{v,i}^{n+1} = T_{v,i}^{n} + \frac{1}{c_{v,i}\rho_{v,i}h_{v,i}}\left\{\Phi_{v,i} + k_{v,i}\frac{2(T_{i+1}^{n} - T_{i}^{n})}{h_{v,i+1} + h_{v,i}} + k_{v,i}\frac{2(T_{i-1}^{n} - T_{i}^{n})}{h_{v,i-1} + h_{v,i}} - \dot{m}_{ev,v}\cdot H_{fg}\right\}\Delta t$$

$$\text{for } i = 2, \ldots, N-1 \tag{28}$$

Also for conventional hot platen pressing, Eq.(28) can be further simplified to:

$$T_{v,i}^{n+1} = T_{v,i}^{n} + \frac{1}{c_{v,i}\rho_{v,i}h_{v,i}}\left\{k_{v,i}\frac{2(T_{i+1}^{n} - T_{i}^{n})}{h_{v,i+1} + h_{v,i}} + k_{v,i}\frac{2(T_{i-1}^{n} - T_{i}^{n})}{h_{v,i-1} + h_{v,i}} - \dot{m}_{ev,v}\cdot H_{fg}\right\}\Delta t$$

$$\text{for } i = 2, \ldots, N-1 \tag{29}$$

EXPERIMENTAL PROCEDURES

Materials

Poplar veneers with a thickness of 1.7 mm were obtained from a plywood mill located in Linyi, Shandong (China). They were selected from the top-grade stacks, which have the smallest thickness variations and relatively better appearance. These veneers sheets were cut to a small area size (470×470 mm) and conditioned in a chamber with a temperature of 20±3 °C and a relative humidity of 65±5% until they reached a constant weight. The final MC of the conditioned veneer sheets was about 12%.

After the preconditioning process, 186 small veneer sheets (470×470×1.7 mm) were randomly selected. Four specimens were cut along the grain direction from each

veneer sheet for measuring the average initial MC. One group of 93 veneer sheets was used to make 31-ply LVL panels with three replicates; the other group of 93 veneers were used for veneer HF heating without compression (drying) with three replicates.

Commercial PF glue (Dynea Co., Ltd, Nanjing, China) with the solids content of 45% was used to make LVL panels by HF heating. Glue application of 120 g/m^2 per single glueline was conducted by a glue spreader. The target panel compression ratio (CR) was 5%.

Equipment Set-up

The apparatus for HF heating applications was composed of an HF generator, a press, a dielectric material, and a temperature sensor system, as shown in Fig. 3. The sensor system consisted of several optic fiber temperature sensors (OFTSs), which were attached to a collecting box that was connected to a personal computer (PC). Temperature readings were automatically recorded by the PC every 10s. The assembly heating was carried out using an HF generator (CGYJ-150D; Shijiazhuang Cangao High Frequency Machinery Co., Ltd, Shijiazhuang, China) with a power output of 30kW and a standard frequency of 6.78MHz. The top and bottom platens both consisted of one plywood panel and one electrode. A plywood panel with a thickness of 500 mm was used as one thermal insulator to reduce the heat loss during HF heating.

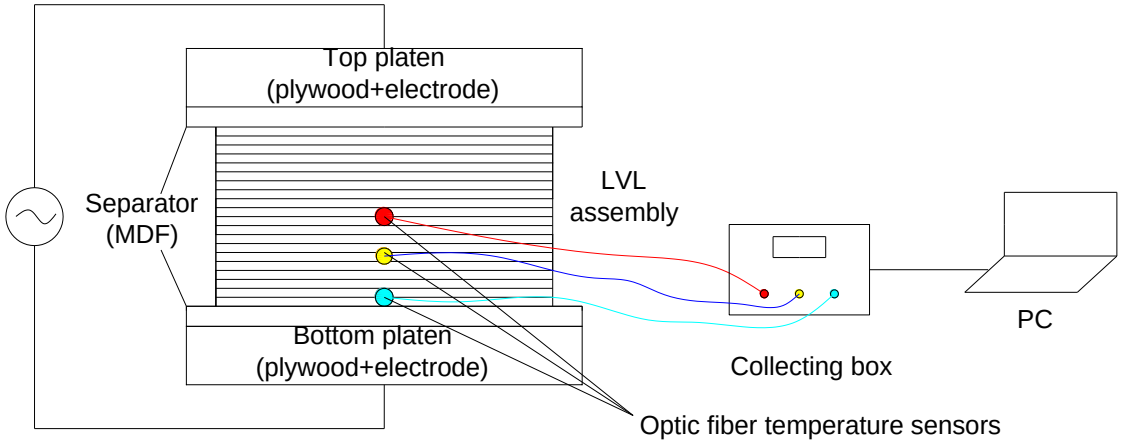

Fig. 3. Schematic representation of the LVL panel HF heating apparatus

LVL HF Heating with Compression

Glue-coated veneer sheets were consolidated under heat and compression with a CR of 5%. At this CR, gas movement and heat convection were negligible because of the significant reduction of veneer permeability (Wang 2007). The temperature inside the panel influenced the glue curing time and in turn determined the manufacturing efficiency. Therefore, the temperature increase of the LVL assembly was the primary concern in this work.

Before each experiment, the HF press required some adjustments. Three OFTSs were inserted into the three special grooves (at z=0, z=h/4 *and* z=h/2). A thickness control was adopted in this experiment; in other words, the electrodes were placed close to the target panel thickness, and this distance remained unchanged. Two sheets of medium density fiber board (MDF) with a thickness of 22 mm were placed between the electrode and the LVL assembly as a separator to avoid arcing from glue squeezed out at the edges of the assembly.

Veneer HF Heating without Compression (*i.e.*, drying)

Because of the consolidation of veneer layers and glue, the moisture change (*i.e.*, mass transfer) of each veneer sheet was difficult to measure. Therefore, one experiment on veneer HF heating without compression (*i.e.*, drying) was designed to investigate the moisture mass transfer. Veneer sheets (31 in total) were laminated without glue; the sheets were all aligned in the same grain direction and then placed into the HF press for heating. In this experiment, only one fiber optic temperature sensor was inserted into the central layer of the assembly. After heating, the weight of each veneer sheet was immediately measured to calculate the mass loss and MC.

RESULTS AND DISCUSSION

Validation of Heat Transfer during LVL HF Heating

As shown in Fig. 4, because of the existence of the thermal insulators, the predictions of temperature *versus* heating time at three different locations were identical; thus, only the prediction for location $z=h/2$ was chosen to present. This theoretically illustrated that the HF heating of a dielectric material exhibited a uniform temperature distribution under the special boundary condition. Based on the comparison of the experimental and predicted results, the mathematical model (Eq. 28) can be used to accurately simulate the HF heating behavior of the LVL assembly.

The experimental results showed that the temperature trend was slightly different at the three locations; namely, the location at the boundary ($z=0$) had the lowest temperature when compared to the other two locations. This temperature difference with real-time measurement was caused by heat loss at the boundaries.

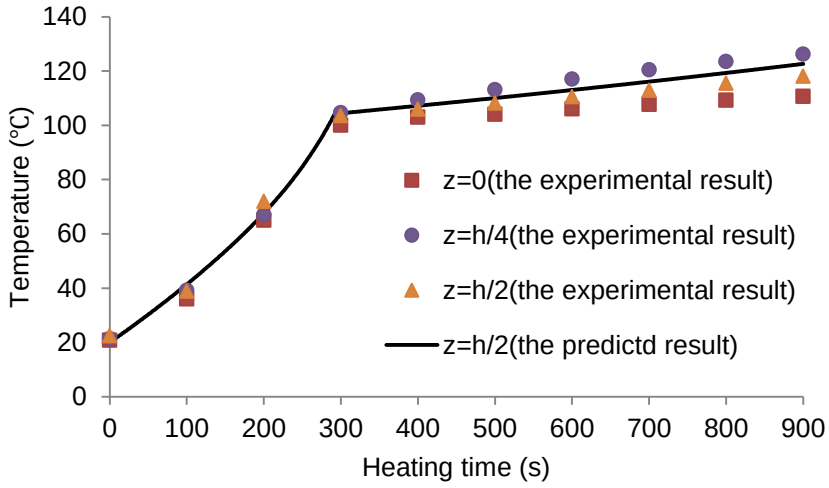

Fig. 4. Comparison of the experimental and numerical results

Another interesting phenomenon was that the experimental curves leveled off when the temperature reached about 100 °C. This could be primarily attributed to the phase change of liquid water in the veneers and glue. Glue polymerization could be a secondary contributor. As the glue cured, the liquid water in the glue also evaporated. This water evaporation would consume a significant amount of energy, and the reduction of the liquid water and the increase in the glue polymerization could reduce the dielectric

loss of the material, which in turn, reduced the absorption power of the material. In addition, the energy loss caused from water vapor escaping from the edges of the LVL assembly also affected the temperature increase. Nevertheless, the mathematical model curves were able to predict this observed phenomenon.

In general, during conventional hot platen heating, the low thermal conductivity of wood is an impediment to heat transfer. As shown in Fig. 5, based on the model predictions, the temperature at the boundary (z=0) rose rapidly within a short amount of time to approximately 130 °C and then slowly leveled off at the target temperature. As the heat transferred from the surface to the inner core of the LVL assembly, the temperature at $z=h/4$ gradually increased, whereas the temperature at the center ($z=h/2$) took an extremely long time to reach the required glue curing temperature. However, the predicted core temperature rise of the LVL assembly was very different during HF heating. According to Eqs. 17 and 20, both the dielectric loss of the material and the absorbed power of the material increased exponentially with temperature and MC. At the early stage of HF heating, the MC could be assumed to be unchanged, but the temperature increased quickly. This temperature increase caused a drastic increase in absorbed power, which led to a higher rate of temperature rise. The temperature increase would then level off due to the phase change of water and glue polymerization, as discussed earlier. HF heating could thus significantly reduce the heating cycle and offer a robust method for making thicker veneer-based composites.

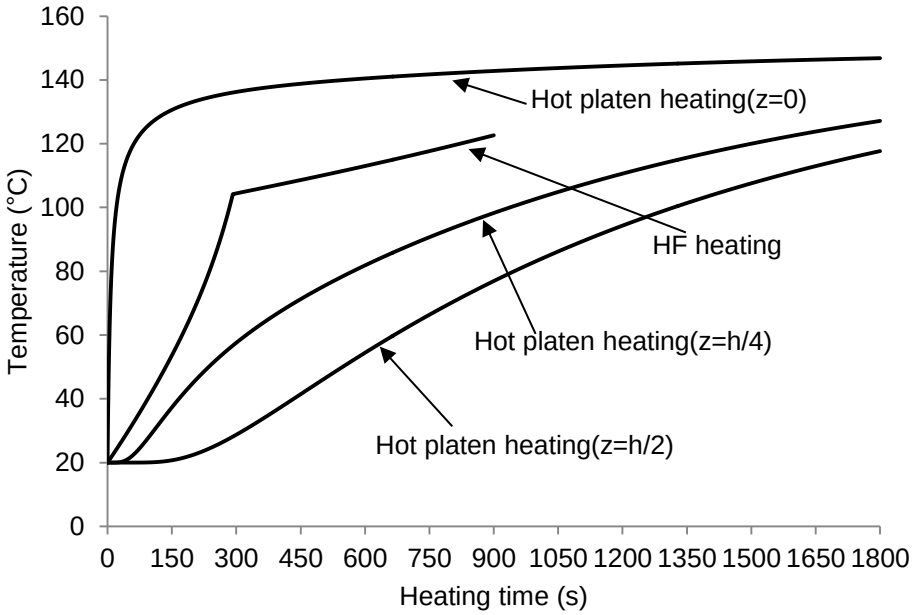

Fig. 5. Temperature increase prediction for the LVL assembly during conventional hot platen heating *versus* HF heating

Validation of Heat and Mass Transfer during HF Heating of a Veneer Assembly without Compression

Figure 6 illustrates the averaged results from three experimental replicates for the MC changes of each veneer sheet after 6 min of HF heating without compression (*i.e.*, drying). The MC of each veneer after heating decreased; however, one interesting phenomenon observed was that the MC reduction of surface layers was slightly lower than that of the core layer. The gas movement was obvious when there was no

compression on the veneer assembly, as discussed above. It is well known that the heat transfer inevitably causes the migration of moisture, or *vice versa*. Water vapor transfer was driven by the local gas pressure, which was also temperature dependent. Where the temperature was high, the gas pressure was also high. Thus, the higher gas pressure forced the water vapor to migrate to a zone with lower gas pressure. Because the heat loss was impossible to avoid between the assembly and the cold metallic electrodes, the temperature rise rate of the surface layers was somewhat lower than that of the core layers. Thus, water vapor movement was driven from the inner core layers to the surface layers, which resulted in the inner core layers having lower MC. Additionally, water vapor escaping from the edges of the assembly led to a MC reduction for each veneer sheet.

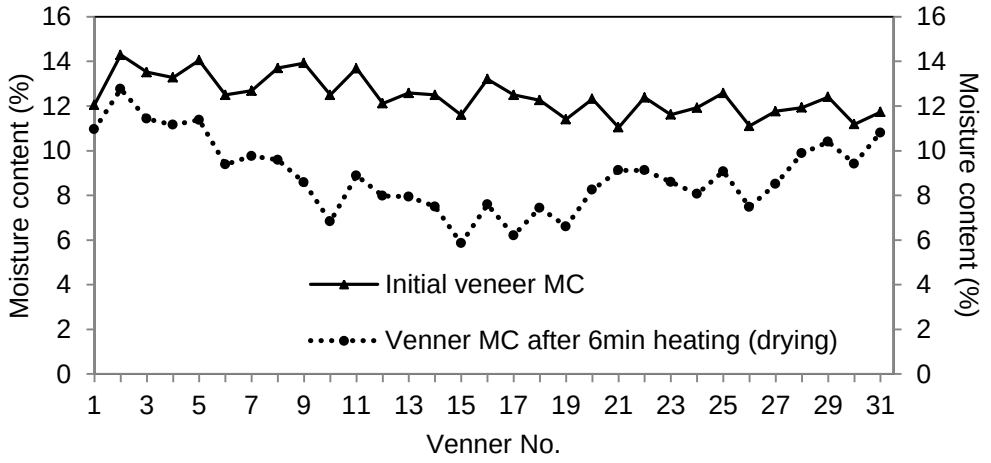

Fig. 6. MC change of each veneer sheet after 6min of HF heating (drying)

Figure 7 shows the comparison of the MC of each veneer sheet experimentally measured, as well as predicted by the developed model (Eq. 23). Because of the experimental errors, the measured results were not absolutely identical to the predicted results. However, the moisture mass transfer trend was well represented by the model.

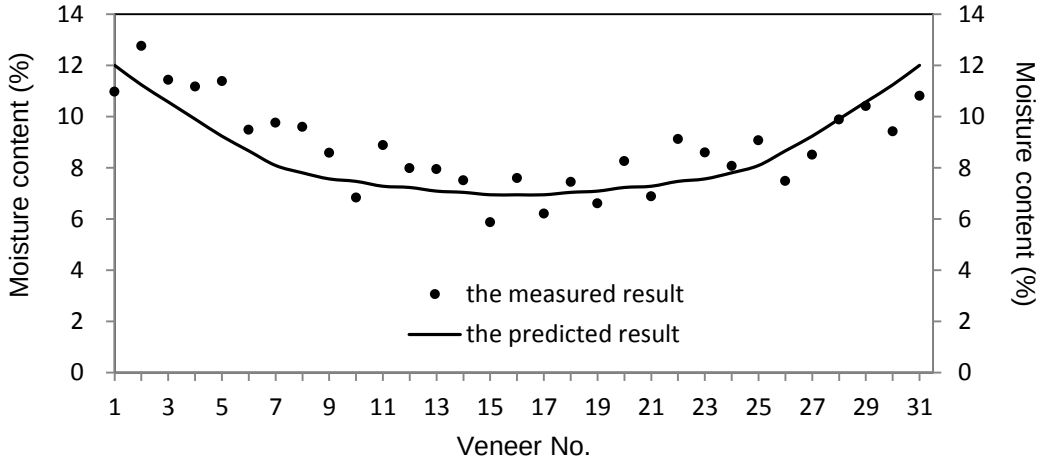

Fig. 7. Comparison of experimentally measured and model-predicted veneer MC

Figure 8 shows the comparison of the temperature experimentally measured and the model predicted at the central location ($z=h/2$) of the veneer assembly based on Eq.(22). Obviously, the predicted model results agreed very well with the experimental values.

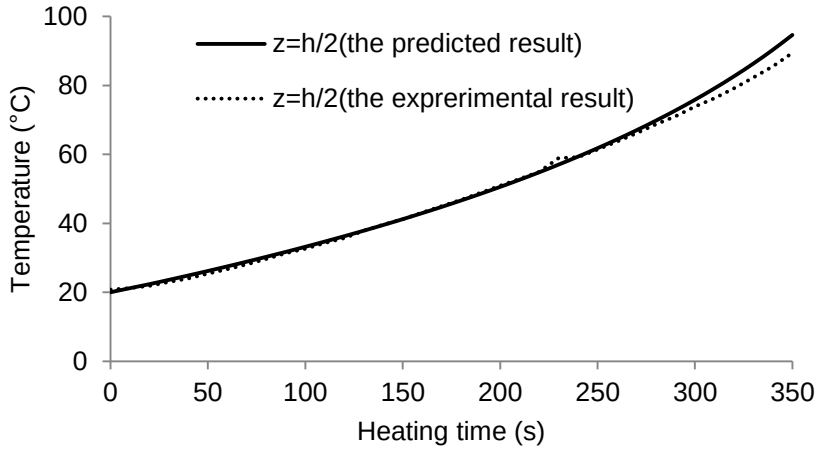

Fig. 8. Comparison of the model-predicted and experimentally measured results

These comparisons demonstrated that the model can also represent the temperature and MC changes in veneer sheets during HF heating without compression.

CONCLUSIONS

1. A one-dimensional mathematical model for heat and mass transfer of HF heating of veneer-based composites was developed. This model describes the coupled physical phenomena that occur during HF heating of veneer-based composites in terms of energy, mass, and momentum conservation. During HF heating, the heat transfer is primarily heat conduction dependent and the absorbed EM energy is the main energy source.
2. In this study, the contribution of heat convection during HF heating of veneer-based composites was first discussed; the results showed that heat convection or gas movement along the vertical direction should be negligible when a CR of 5 to 15% is employed during the manufacturing of veneer-based composites. And then the model was further simplified.
3. Two experiments were conducted to validate the model. The experimental results showed that the model could be successfully used to predict the heat transfer of veneer-based composites during HF heating with compression, and heat and mass transfer of a veneer assembly during HF heating without compression (*i.e.*, drying). During HF heating without compression (*i.e.*, drying) of the veneer assembly, the inner core veneer layers had a lower MC than the outer surface veneer layers.
4. Compared with the conventional hot platen heating, HF heating was theoretically and experimentally demonstrated to be an efficient and robust method for manufacturing thick veneer-based composites.

ACKNOWLEDGMENTS

The authors are grateful for the support of the National Twelfth Five-Year Science and Technology Project (2012BAD24B010205), the National Forestry Public Industry Research Fund (201104004), and the Priority Program Development of Jiangsu Higher Education Institutions (PAPD). Additionally, Dr. P. Wei would like to thank FPInnovations for supporting this work.

REFERENCES CITED

Bolton, A., and Humphrey, P. (1994). "The permeability of wood-based composite materials. Part1. A review of the literature and some unpublished work," *Holzforschung* 48(1), 95-100.

Bolton, A., Humphrey, P., and Kavvouras, P. (1989a). "The hot pressing of dry-formed wood-based composites: Part III. Predicted vapor pressure and temperature variation with time, and compared with experimental data for laboratory board," *Holzforschung* 43(4), 265-274.

Bolton, A., Humphrey, P., and Kavvouras, P. (1989b). "The hot pressing of dry-formed wood-based composites: Part IV. Predicted variation of mattress moisture content with time," *Holzforschung* 43(5), 345-349.

Bucki, M., and Perré, P. (2003). "Physical formulation and numerical modeling of high frequency heating of wood," *Drying Technol.* 21(7), 1151-1172.

Carvalho, L., and Costa, C. (1998). "Modeling and simulation of the hot pressing process in the production of MDF," *Chem. Eng. Comm*. 170(1), 1-21.

Cheng, J. (1985). *Wood Science*, China Forestry Press, Beijing, China (in Chinese).

Dai, C. (2001). "Viscoelastic behaviors of wood composite mats during consolidation," *Wood Fiber Sci.* 33(3), 353-363.

Dai, C., and Yu, C. (2004). "Heat and mass transfer in wood composite panels during hot pressing: Part I. A physical-mathematical model," *Wood Fiber Sci*. 36(4), 585-597.

Dai, C., Yu, C., and Zhou, X. (2005). "Heat and mass transfer in wood composite panels during hot pressing: Part II. Modeling void formation and mat permeability," *Wood Fiber Sci.* 37(2), 242-257.

Dai, C., Yu, C., Xu, C., and He, G. (2007). "Heat and mass transfer in wood composite panels during hot pressing: Part 4. Experimental investigation and model validation," *Holzforschung* 61(1), 74-82.

Deng, J., Xie, Y., and Feng, M. (2006). "An experimental study of microwave pre-heating of an MDF fibre mat: Moisture and temperature distribution and the impact on hot-pressing," *For. Prod. J.* 56(6), 76-81.

Fahey, D. (1976). "High frequency pressing of phenolic-bonded hardboards," *For. Prod. J.* 27(7), 32-33.

von Haas, G., and Fruhwald, A. (2000). "Compression behavior of fiber, particle and strand mats," *Holz. Roh. Werkst.* 58(5), 317-323.

von Haas, G., and Fruhwald, A. (2001). "Rheological behavior of fiber, particle and strand mats," *Holz. Roh. Werkst*. 58(6), 415-418.

von Haas, G., Steffen, A., and Fruhwald, A. (1998). "Permeability of fiber, particle and strand mats for gas," *Holz. Roh. Werkst.* 56(6), 386-392.

Humphrey, P., and Bolton, A. (1989). "The hot pressing of dry-formed wood-based composites: Part II. A simulation model for heat and moisture transfer, and typical results," *Holzforschung* 43(3), 199-206.

James, W. (1977). "Dielectric behavior of Douglas-fir at various combinations of temperature, frequency, and moisture content," *For. Prod. J.* 27(6), 44-48.

Jones, P., and Rowley, A. (1996). "Dielectric drying," *Drying Technol.* 14(5), 1063-1098.

Incropera, F., and Dewitt, D. (1990). *Fundamentals of Heat and Mass Transfer*, 3rd Ed., John Wiley & Sons, New York.

Kelly, M. (1977). "Critical review of relationship between processing parameters and physical properties of particleboard," General Technical Report FPL-10, U.S. Department of Agriculture, Forest Service, Forest Products Laboratory, Madison, WI, 65 pp.

Kröner, K., and Pungs, L. (1953). "Über das verhalten des dielektrischen verlustfaktors vonnaturholz im großen frequenz bereich," *Holzforschung* 7(1), 12-18.

Lenth, C., and Kamke, F. (1996). "Investigations of flakeboard mat consolidation. Part II. Modeling mat consolidation using theories of cellular materials," *Wood Fiber Sci*. 28(3), 309-319.

Lu, C. (1986). *The Relationship between High Frequency Heating and Performance of LVL Made from Small Diameter Larch*, Ph.D. Diss., Northeast Forestry University, Harbin, China (in Chinese).

Maloney, T. (1989). *Modern Particleboard & Dry-Process Fiberboard Manufacturing.* Miller Freeman Publication, San Francisco, CA, USA, 672 pp.

Nelson, R. (1983). "A model for sorption of water vapor by cellulosic materials," *Wood Fiber Sci.* 15(1), 8-22.

Odian, G. (2004). *Principles of Polymerization, 4th Edition*, John Wiley & Sons, New York, NY, 832 pp.

Pereira, C., Blanchard, C., Carvalho, L., and Costa, C. (2004). "High frequency heating of medium density fiberboard (MDF): Theory and experiment," *Chem. Eng. Sci.* 59(4), 737-745.

Pound, J. (1959). "The effect of moisture on RF heating," *Wood* 24(11), 452-455.

Resch, H. (2006). "High-frequency electric current for drying of wood-historical perspectives," *Maderas - Cienc.Tecnol.* 8(2), 67-82.

Resnik, J., Šernek, M., and Kamke, F. (1997). "High-frequency heating of wood with moisture content gradient," *Wood Fiber Sci*. 29(3), 264-271.

Roussy, G., and Pearce, J. (1995). *Foundations and Industrial Applications of Microwaves and Radio Frequency Fields: Physical and Chemical Processes*, John Wiley & Sons, New York, NY, 492 pp.

Sernek, M., and Kamke, F. (2007). "Application of dielectric analysis for monitoring the cure process of phenol formaldehyde adhesive," *Int. J. Adhes. Adhes.* 27(7), 562-567.

Shen, Z. (1983). *Wood Science*, China Forestry Press, Beijing, China (in Chinese).

Siau, J. (1995). *Wood: Influence of Moisture on Physical Properties*, Department of Wood Science and Forest Products, Virginia Polytechnic Institute and State University, Blacksburg, VA, 227 pp.

Thöemen, H., and Humphrey, P. (2003). "Modeling the continuous pressing process for wood-based composites," *Wood Fiber Sci.* 35(3), 456-468.

Thöemen, H., and Humphrey, P. (2006). "Modeling the physical processes relevant during hot pressing of wood-based composites. Part I. Heat and mass transfer," *Holz. Roh. Werkst*. 64, 1-10.

Torgovnikov, G. (1993). *Dielectric Properties of Wood and Wood-Based Materials*, Springer-Verlag, Berlin, Germany, 196 pp.

Wang, B.J. (2007). *Experimentation and Modelling of Hot Pressing Behavior of Veneer-Based Composites*, Ph.D. Diss., The University of British Columbia, Vancouver, BC, Canada.

Wang, B.J., Zhou, X., Dai, C., and Ellis, S. (2006). "Air permeability of aspen veneer and glueline: Experimentation and implication," *Holzforschung* 60(3), 304-312.

Wang, P., and Winstorfer, P. (2000). "Consolidation of flakeboard mats under theoretical laboratory pressing and simulated industrial pressing," *Wood Fiber Sci.* 32(4), 527-538.

Woodson, G., and Stevens, R. (1977). "High-frequency and hot-platen curing of medium-density fiberboards," *For. Prod. J.* 27(1), 46–50.

Yin, S. (1996). *Wood Science*, China Forestry Press, Beijing, China (in Chinese).

Yu, C. (2011). *Numerical Analysis of Heat and Mass Transfer for Porous Materials*, Tsinghua University Press, Beijing, China (in Chinese).

Yu, C., Dai, C., and Wang, B.J. (2007). "Heat and mass transfer in wood composite panels during hot pressing: Part 3. Predicted variations and interactions of pressing variables," *Holzforschung* 61(1), 74-82.

Zombori, B., Kamke, F., and Watson, L. (2002). "Simulation of the internal conditions during the hot-pressing process," *Wood Fiber Sci.* 35(1), 2-23.

Article submitted: January 21, 2014; Peer reviews (previous part 1) completed: March 27, 2014; Part 2 review input sent to authors: March 28, 2014; Article's combined and revised version received and accepted: April 11, 2014; Published: April 21, 2014.